available at www.sciencedirect.com

ScienceDirect

journal homepage: www.elsevier.com/locate/biochempharm

C421 allele-specific ABCG2 gene amplification confers resistance to the antitumor triazoloacridone C-1305 in human lung cancer cells

Eran E. Bram [a], *Ilan Ifergan* [a], *Michal Grimberg* [a], *Krzysztof Lemke* [b], *Andrzej Skladanowski* [b], *Yehuda G. Assaraf* [a,*]

[a] *The Fred Wyszkowski Cancer Research Laboratory, Faculty of Biology, Technion-Israel Institute of Technology, Haifa 32000, Israel*
[b] *Laboratory of Cellular and Molecular Pharmacology, Department of Pharmaceutical Technology and Biochemistry, Gdansk University of Technology, Gdansk, Poland*

ARTICLE INFO

Article history:
Received 29 December 2006
Accepted 22 March 2007

Keywords:
Chemotherapy
ABC transporter
Efflux pumps
Drug resistance

ABSTRACT

The A421 ABCG2 genotype is a frequent polymorphism encoding the K141 transporter, which is associated with a significant decrease in transporter expression and function when compared to the wild type (wt) C421 allele encoding the Q141 ABCG2. Here we show that during the acquisition of resistance to the novel triazoloacridone antitumor agent C-1305 in lung cancer cells harboring a heterozygous C421A genotype, a marked C421 allele-specific ABCG2 gene amplification occurred. This monoallelic C421 ABCG2 gene amplification brought about the overexpression of both C421 ABCG2 mRNA and the transporter at the plasma membrane. This resulted in the lack of cellular drug accumulation due to increased efflux of both C1305 and C-1311, a fluorescent imidazoacridone homologue of C-1305, as well as marked resistance to these antitumor agents and to established ABCG2 substrates including mitoxantrone and SN-38. Consistently, the accumulation and sensitivity to these drugs were restored upon incubation with the potent and specific ABCG2 transport inhibitors Ko143 and fumitremorgin C. Moreover, upon transfection into HEK293 cells, the wt Q141 ABCG2 allele displayed a significantly decreased accumulation of C-1311 and increased resistance to C-1305, C-1311 and mitoxantrone, when compared to the K141 ABCG2 transfectant. Hence, the current study provides the first evidence that during the exposure to anticancer drugs, an allele-specific Q141 ABCG2 gene amplification occurs that confers a drug resistance advantage when compared to the K141 ABCG2. These findings have important implications for the selection and expansion of malignant anticancer drug resistant clones during chemotherapy with ABCG2 drugs.

© 2007 Elsevier Inc. All rights reserved.

1. Introduction

Despite enormous efforts, the achievement of curative cancer chemotherapy has been at best partially successful, particularly for the treatment of the frequent solid tumors of the lung, breast, prostate and colon. In a search for novel acridine-based antineoplastic agents, a series of triazoloacridones with potent antitumor activity *in vivo* against a range of murine and human

* *Corresponding author*. Tel.: +972 4 829 3744; fax: +972 4 822 5153.
E-mail address: assaraf@tx.technion.ac.il (Y.G. Assaraf).

Abbreviations: MDR, multidrug resistance; ABC, ATP-binding cassette; BCRP, breast cancer resistance protein; MRP, multidrug resistance protein; Pgp, P-glycoprotein

0006-2952/$ – see front matter © 2007 Elsevier Inc. All rights reserved.
doi:10.1016/j.bcp.2007.03.028

tumors were developed [1]. C-1305, the most potent triazoloacridone derivative, achieved complete cures for the majority of animals bearing colon carcinoma xenografts [2].

The structural similarity of C-1305 with established topoisomerase II inhibitors including mitoxantrone and amsacrine (m-AMSA) (Fig. 1) suggested that C-1305 is a potential topoisomerase II inhibitor. Indeed, it has been recently shown that C-1305 is a topoisomerase II poison that induces the formation of potent cleavable complexes that are selectively toxic toward tumor cells which have lost the function of the tumor suppressors p53 and/or p21 [3]. This finding is of particular importance as the p53 tumor suppressor is frequently inactivated in human tumors including colorectal cancers [4]. Previous studies have shown that C-1305 binds to DNA by intercalation and consequently induces unique structural perturbations in DNA regions with three adjacent guanine residues [5]. This unique effect was highly specific for C-1305 as none of the 22 different DNA interacting drugs and topoisomerase II inhibitors tested was able to induce similar structural alterations. Molecular modeling revealed that the zwitterionic form of C-1305 intercalates within the guanine triplet, resulting in widening of both DNA grooves and aligning of the triazole ring with the N-7 atoms of the guanines.

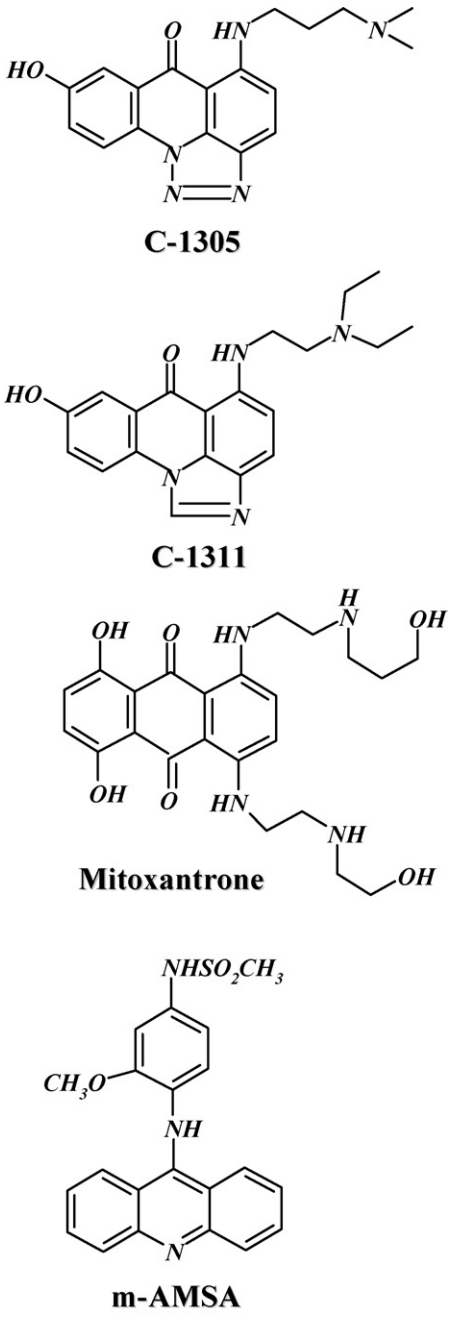

Fig. 1 – Chemical structures of the topoisomerase II inhibitors C-1305, C-1311, mitoxantrone and m-AMSA.

One of the best-characterized mechanisms of anticancer drug resistance is multidrug resistance (MDR) mediated by ATP-driven drug efflux transporters [for reviews see [6–13]]. Currently, 49 human ABC genes have been identified [14] including the MDR transporters which are plasma membrane glycoproteins conferring resistance to a wide spectrum of anticancer drugs in malignant cells. At the physiological level, these ABC transporters play an important protective role against a multitude of toxicants and in a variety of tissues, particularly in secretory and absorptive epithelia as well as in blood-tissue barriers including the blood-brain barrier. The three major MDR transporters are ABCB1 (Pgp, MDR1) [7,9], ABCC1 (MRP1) [6,10,13,15] and ABCG2 (BCRP/ABCP/MXR) [8,11–13,15]. ABCB1 and ABCC1 transport a large array of structurally unrelated hydrophobic cytotoxic drugs and in addition, ABCC1 can also extrude anionic drugs and anionic conjugates. Similarly, the transport properties of ABCG2 overlap to some extent those of ABCB1 and several MRPs, the latter of which currently encompass nine members including ABCC1 through ABCC10 (MRP7) as well as ABCC11 and ABCC12 [16]. Hence, these three primary groups of MDR efflux transporters including ABCB1, ABCC1 and ABCG2 form a unique defense network against multiple chemotherapeutic agents and cellular toxicants.

Here we studied the molecular basis of C-1305 resistance in cultured A549 human non-small cell lung cancer cells. We find that the acquisition of C-1305 resistance was associated with Q141 allele-specific ABCG2 gene amplification and its functional overexpression at the plasma membrane. This consequently resulted in an efficient drug extrusion and resistance to various drugs that are established ABCG2 transport substrates. Since the K141 allele has been associated with markedly decreased ABCG2 expression and function [17,18], our results provide the first evidence that during the acquisition of drug resistance, the ABCG2 gene may undergo a Q141 monoallelic gene amplification thereby ensuring its efficient overproduction and efflux activity. These findings reinforce the pivotal role ABCG2 plays in mediating anticancer drug resistance and provides a paradigm for an advantageous malignant clonal selection and expansion during chemotherapy with ABCG2 type drugs.

2. Materials and methods

2.1. Drugs and chemicals

Triazoloacridone C-1305, imidazoacridone C-1311 (Symadex®) and amsacrine (m-AMSA) were synthesized by Dr. B. Horowska and Dr. M. Konieczny at the Dept. of Pharmacological

Technology and Biochemistry, Gdansk University of Technology, Poland. Ethylmethane sulfonate, [3-(4,5-dimethylthiazol-2-yl)-2,5-diphenyltetrazolium bromide] (MTT). G-418 and various cytotoxic agents were from Sigma–Aldrich Inc., St. Louis, Missouri. Ko143 was kindly provided by Prof. A.H. Schinkel, Netherlands Cancer Institute, Amsterdam, The Netherlands, whereas fumitremorgin C and SN-38 were a generous gift of Dr. S.E. Bates, National Cancer Institute, Bethesda, MD.

2.2. Tissue culture

Human A549 non-small cell lung cancer cells were grown under monolayer conditions in RPMI-1640 medium (Invitrogen™-GIBCO® Carlsbad, CA) containing 10% fetal calf serum, 2 mM glutamine, 100 μg/ml penicillin and 100 μg/ml streptomycin (Biological Industries, Beth-Haemek, Israel) in a humidified atmosphere of 5% CO_2. The human ovarian carcinoma cell line 2008 and its MRP3 stably transduced subline 2008/MRP3 (kindly provided by Prof. P. Borst, The Netherlands Cancer Institute, Amsterdam, The Netherlands) [19], was cultured as above. Human embryonic kidney cells (HEK293) and their stable transfectants overexpressing the WT Q141- and the polymorphic K141 ABCG2 (kindly provided by Dr. S.E. Bates) [18] were grown as described above. The growth medium of the Q141- and K141 ABCG2 transfectants was routinely supplemented with 2 mg/ml G-418.

2.3. Development of C-1305 resistant cells

C-1305-resistant A549/K1.5 cells were established from parental A549 cells by mutagenesis with a single dose exposure of cells ($\sim 3 \times 10^6$) to 7.5 mM ethylmethane sulfonate for 18 h followed by a continuous incubation with gradually increasing concentrations of C-1305 until cells were able to normally proliferate at 1.5 μM C-1305 (a total of ~4 months). One clone termed A549/K1.5 displaying a stable drug resistance phenotype for at least 6 months of growth in drug-free medium was chosen for further characterization.

2.4. RNA extraction and ABCG2 nucleotide sequence analysis

Total RNA was extracted using the TriReagent protocol (Sigma–Aldrich Inc., St. Louis, MO). cDNA synthesis was carried out using 12 μg of RNA in a 50 μl reaction mixture containing random hexamer primers and mMLV reverse transcriptase at 37 °C (Promega Corporation, Madison, WI). ABCG2 PCR primers (Table 1) were designed using the GeneRunner Version 3.00 software (Hastings Software, Inc.), in accordance with the human ABCG2 NM_004827 RefSeq. PCR was performed in a total volume of 50 μl in the presence of 100 ng of cDNA, 0.4 μM of primers and a 1× RedTaq™ ReadyMix™ PCR reaction mix solution (Sigma–Aldrich Inc., St. Louis, MO). Following an initial denaturation at 95 °C for 10 min, 35–40 cycles each of 1 min denaturation at 95 °C, 1 min annealing at 53–62 °C and 1 min elongation at 72 °C, as well as a final extension period of 10 min at 72 °C, were carried out. Purification of PCR products from agarose gels or PCR reactions was performed using the Wizard® SV Gel and PCR Clean-Up System (Promega Corporation, Madison, WI).

2.5. Quantification of ABCG2 gene expression by semi-quantitative RT-PCR and real-time PCR analyses

To evaluate the level of ABCG2 gene expression, a semi-quantitative RT-PCR method was used. Two alternative

Table 1 – Primers used throughout the current study and their amplicon characteristics

Primer#	Sense	Anti-sense	Fragment localization in reference sequence	Size (bp)	T_m (°C)
Semi-quantitative RT-PCR and transcript sequence					
ABCG2 (NM_004827 CDS)					
1	5′-CTGAGCTCGTCCCCTGGATG-3′	5′-GCTATCGAGTAAAACTGAAGAGTGGC-3′	−483 to 153	636	61
2	5′-GTCACAAGGAAACACCAATGG-3′	5′-CCAGACACACCACGGATAAACTG-3′	36–563	528	62
3	5′-CAGTTCTCAGCAGCTCTTCGGC-3′	5′-GGAAGGCTCTATGATCTCTGTGGC-3′	421–966	546	62
4	5′-GCTGGTTATCACTGTGAGGCC-3′	5′-CTGCCTTTGGCTTCAATC-3′	838–1510	673	55
5	5′-GATTG AAGCCAAAGGCAG-3′	5′-CAGGTAGGCAATTGTGAG-3′	1493–1938	446	53
6	5′-GCATCTTGGCTGTCATGGC-3′	5′-GCTGTGCAACAGTGTGATGGC-3′	1684–2085	402	60
β-Actin (NM_001101 CDS)					
1	5′-CCGTCTTCCCCTCCATCGTG-3′	5′-GGGCGACGTAGCACAGCTTCT-3′	86–661	576	62
Semi-quantitative genomic PCR and sequence of C421A SNP					
ABCG2 (NC_000004)					
1	5′-GGGTGTACAGATAGGGGGTG-3′	5′-GACCCTGTTAATCCGTTCG-3′	89,271,276–89,271,602	325	57
2	5′-AAACAGTCATGGTCTTAGAAAAG-3′	5′-TCTCATTGTTATGGAAAGCAACC-3′	89,271,106–89,271,455	350	53
β-Actin (NC_000007)					
1	5′-CGTTGCTATCCAGGCTGTGC-3′	5′-GCCAGCCAGGTCCAGACGC-3′	5,534,694–5,534,841	148	60
Quantitative real time RT-PCR					
ABCG2 (NM_004827 CDS)					
1	5′-CCCGCGACAGCTTCCAATGA-3′	5′-GGCGTTGAGACCAGGTTTCA-3′	61–231	171	60
β-Actin (NM 001101 CDS)					
1	5′-CATGTACGTTGCTATCCAGGC-3′	5′-CTCCTTAATGTCACGCACGAT-3′	393–642	250	60
GAPDH (NM_002046 CDS)					
1	5′-ATGGGG AAGGTGAAGGTCG-3′	5′-GGGGTCATTGATGGCAACAATA-3′	1–108	108	60

human ABCG2 PCR products (fragments 3 and 4, Table 1) were obtained by PCR amplification after 25–30 cycles as described above, using two-fold serial template dilutions in a 25 μl reaction mixture. Prior to RT-PCR, the A549/K1.5 cDNA template was pre-diluted by a factor of 32-fold. β-Actin (primers depicted in Table 1) was used as an endogenous reference gene. Representative results of three independent experiments are shown.

ABCG2 mRNA levels were also determined by SYBR Green quantitative real-time PCR using an ABI Prism 7000 sequence detection system (Applied Biosystems, Foster City, CA). Quantitative PCR reactions (20 μl) contained 50 ng of cDNA, 70 nM of the primers and 1× Absolute™ QPCR SYBR Green Mix universal PCR master mix (Applied Biosystems, Foster City, CA). Results represent means ± S.D. of three independent experiments.

2.6. Determination of allele-specific ABCG2 gene amplification by genomic PCR and sequencing

Genomic DNA was extracted using the TriReagent protocol and PCR was performed as described above for semi-quantitative RT-PCR. The genomic primers used in this assay are those depicted in Table 1. This revealed 325 bp or 350 bp fragments located in exon 5 of the ABCG2 gene including the polymorphic C421A nucleotide. PCR products were either directly sequenced or TA-cloned into the pGEM®-T Easy Vector System (Promega Corporation, Madison, WI). Approximately 38 positive genomic PCR clones from each cell line were picked, amplified, sequenced and the frequency of ABCG2 nucleotide polymorphism at position 421 was determined. ABCG2 cDNA sequencing was performed using an ABI Prism 310 DNA Sequencer (AME Bioscience, Toroed, Norway).

2.7. Western blot analysis of ABCG2 and MDR transporter expression

To determine the expression of ABCG2, ABCC1 through ABCC5, as well as ABCB1 in the various cell lines, protein extraction and Western blot analysis were performed as previously described [20]. Briefly, following SDS polyacrylamide gel electrophoresis and electroblotting, blots were blocked and reacted with the following monoclonal antibodies (generously provided by Prof. R.J. Scheper and Dr. G.L. Scheffer, VU University Medical Center, Amsterdam, The Netherlands): BXP-53 (rat anti-ABCG2; 1:1000), MRP-r1 (rat anti-ABCC1; 1:1000), M_2III-6 (mouse anti-ABCC2; 1:500), M_3II-21 (mouse anti-ABCC3; 1:500), M_4I-80 (mouse anti-ABCC4; 1:500), M_5I-1 (mouse anti-ABCC5; 1:750), and C-219 (mouse anti-ABCB1; 1:250). Blots were then rinsed and reacted for 1 h at room temperature with second antibodies consisting either of horseradish peroxidase (HRP)-conjugated goat anti-mouse or anti-rat IgG (1:10,000; Jackson ImmunoResearch Laboratories, West Grove, PA). Following washes, enhanced chemiluminescence detection was performed according to the manufacturer's instructions (Biological Industries, Beth-Haemek, Israel). Normalization of loading differences was carried out as described previously [21]. The Western blot analyses used here are quantitative as they were performed in a linear range of protein loading and autoradiogram exposure.

2.8. Immunohistochemical localization of ABCG2 in monolayer A549/K1.5 cells

Cells (1×10^4) were seeded in 24-well tissue culture plates (1 ml medium/well) and incubated for 2 days. Fixation and ABCG2 probing were performed as previously described [22,23]. Briefly, monolayer cells were washed, fixed with 4% formaldehyde and endogenous peroxidase activity was neutralized. Fixed cells were then washed, blocked and reacted with anti-ABCG2 BXP-53 monoclonal antibody (1:100). HRP-conjugated goat anti-rat IgG was then added, followed by washes and color development using the chromogen 3,3′-diaminobenzidine. After counter-staining with hematoxylin, cells were examined with a DMIRE2 inverted light microscope equipped with a DC300FX camera (Leica Microsystems, Wetzlar, Germany).

2.9. Determination of drug resistance levels

Cellular sensitivity to various antitumor agents was determined using both the MTT assay [24] and the growth inhibition assay followed by viable cell counting [20–23]. For the MTT assay, cells were seeded at 5×10^3 cells (2 ml medium/well) in 24-well plates. Following an overnight incubation, cells were exposed to different drug concentrations for 120 h. Cellular viability was determined by adding the MTT tetrazolium salt for 4 h at 37 °C, followed by solubilization of the intracellular precipitated formazan in 1 ml DMSO and absorbance was determined by a microplate spectrophotometric reader (ASYS Hitech GmbH, Austria). Drug concentrations inhibiting cell growth by 50% (IC_{50}) were determined using the SlideWrite software (Advanced Graphics Software Inc., Encinitas, CA). Results are means of at least three independent experiments, each performed in duplicates. Growth inhibition assay using various concentrations of C-1305, C-1311, mitoxantrone and SN-38, with or without 5 μM fumitremorgin C were done as previously described [21], with the omission of the poly-D-lysine coating of plates.

2.10. C-1305 accumulation and efflux

Drug accumulation was determined by UV–vis spectroscopy. Briefly, after incubation with C-1305, cells were washed twice in ice-cold PBS and re-suspended at 1×10^6/ml in extraction buffer (50% ethanol, 0.1N HCl). Cellular drug was extracted overnight at 4 °C, supernatants were collected and centrifuged at 1000 × *g* for 5 min at 4 °C and the 418 nm absorbance was determined using a Cary-Bio spectrophotometer (Varian, Inc., Palo Alto, CA). A standard curve was prepared using known concentrations of C-1305 in the extraction buffer and was used to convert absorbance values to actual drug concentrations. Cell volume was measured using Coulter Counter Z2 model (Beckman Coulter, Fullerton, CA). Results are means of at least three independent experiments each performed in duplicates.

2.11. Flow cytometric assay of cellular C-1311 accumulation and correlation to ABCG2 plasma membrane levels in viable cells using the 5D3 monoclonal antibody

One millilitre of aliquots of cell suspension (1×10^6 cells/ml) in growth medium containing 20 mM HEPES at pH 7.3 were

distributed into 1.5 ml polypropylene Eppendorf test tubes. Then, C-1311 was added at various concentrations of 0.1–25 μM. To some test tubes containing 10 μM C-1311, the ABCG2 efflux inhibitor Ko143 was added (0.6 μM). After 1 h of incubation at 37 °C, the test tubes were transferred to ice and centrifuged at 4 °C. Cells were then washed once and resuspended in ice-cold PBS containing 0.1% bovine serum albumin (BSA). A fraction of test tubes containing 10 μM C-1311 ± 5 μM fumitremorgin C were incubated for an additional 30 min at 4 °C with an allophycocyanin (APC)-conjugated 5D3 mouse anti-human ABCG2 monoclonal antibody (R&D Systems Inc., Minneapolis, MN), at a 1:4 dilution in PBS containing 0.1% BSA in a total volume of 100 μl. Non-specific fluorescence was normalized using a control containing only the second antibody (i.e. APC-conjugated mouse IgG, Jackson Immunoresearch Labs, West Grove, PA). Cells were then washed twice, resuspended and kept in the dark at 4 °C until analysis. Cellular fluorescence was determined using a FACSCalibur (BD Bioscience, San Jose, CA, USA) flow cytometer. FL1-H excitation of C-1311 was at 488 nm and emission was collected at 525 nm, whereas FL4-H excitation of APC was at 633 nm and emission at 660 nm. Individual cell ABCG2 fluorescence represented by the FL4-H value was plotted against individual cell fluorescence of the accumulated C-1311 represented by FL1-H fluorescence. C-1311 accumulation in HEK293 ABCG2 (Q141K) transfectant cells was carried out as above with the exceptions of using a C-1311 concentration range of 0.1–10 μM and the use of the alternative ABCG2 efflux inhibitor fumitremorgin C (5 μM) when co-incubated with C-1311.

2.12. Immunofluorescence microscopic assay of plasma membrane ABCG2 and nuclear C-1311 accumulation

Cells (1×10^4/well) were seeded in 24-well tissue culture plates (1 ml medium/well) and incubated for 2 days after which some wells were supplemented with 10 μM C-1311-containing media ±5 μM fumitremorgin C and incubated for 1 h at 37 °C. Cells were then washed twice with ice-cold PBS containing 0.1% BSA and blocked for 10 min at 4 °C with PBS containing 5% BSA. Cells were then washed once with ice-cold PBS containing 0.1% BSA and incubated for 30 min at 4 °C with an affinity-purified 5D3 mouse-anti human ABCG2 monoclonal antibody (1:100; eBioscience). Following washing, cells were incubated in the dark with a secondary phycoerythrin (PE)-conjugated goat-anti-mouse IgG (1:200; Jackson Immunoresearch Labs, West Grove, PA). Unspecific fluorescence was determined using cells that were incubated only with the secondary antibody. Cells were then washed twice and subjected to fluorescence microscopy using a DMIRE2 fluorescence microscope equipped with a DC300FX camera (Leica Microsystems, Wetzlar, Germany).

2.13. Calculations of log P values

The lipophilicity parameter log *P* value was calculated for C-1305 and C-1311 using the SPARC (Predictive Modeling System) online server at the U.S. Environmental Protection Agency (Research Triangle Park, NC) [25]. Calculated log *P* values were obtained for partition of drugs between water and octanol at 25 °C/760 Torr.

Table 2 – Summary of growth inhibition studies on A549 and A549/K1.5 cells upon 72 h exposure to various anticancer drugs in the absence or presence of 5 μM fumitremorgin C (FTC; panel A), or under the MTT assay (panel B)

(A) Drug	IC_{50} (nM)			
	A549		A549/K1.5	
	−FTC	+FTC	−FTC	+FTC
C-1305	166 ± 47 (1.0)	69 ± 29 (1.0)	7351 ± 2075 (44.4)	114 ± 10 (1.6)
C-1311 (Symadex)	42 ± 8 (1.0)	32 ± 2 (1.0)	1241 ± 283 (29.3)	50 ± 13 (1.6)
Mitoxantrone	2.1 ± 0.7 (1.0)	2.3 ± 0.4 (1.0)	187 ± 49 (88.8)	5.3 ± 3.3 (2.4)
SN-38	5.6 ± 1.6 (1.0)	4.3 ± 1.2 (1.0)	648 ± 110 (115.6)	5.4 ± 0.9 (1.3)

(B) Drug	IC_{50} (nM)	
	A549	A549/K1.5
Mitoxantrone	2 ± 1.0 (1.0)	200 ± 140 (94.4)
m-AMSA	140 ± 20 (1.0)	140 ± 30 (1.3)
Etoposide (VP-16)	210 ± 140 (1.0)	550 ± 40 (2.8)
Teniposide (VM-26)	20 ± 17 (1.0)	40 ± 30 (2.2)
Daunorubicin	10 ± 3 (1.0)	20 ± 4 (1.5)
Doxorubicin	8 ± 1.1 (1.0)	10 ± 6 (1.6)
ICRF-187	13,800 ± 2950 (1.0)	35,400 ± 1410 (2.6)
Vincristine	21 ± 12 (1.0)	20 ± 9 (0.95)
Paclitaxel	19 ± 1 (1.0)	20 ± 11 (0.99)
Camptothecin	8.3 ± 1.5 (1.0)	16 ± 3.5 (1.98)
Cisplatinum	2090 ± 1030 (1.0)	2270 ± 502 (1.1)
5-Fluorouracil	2370 ± 240 (1.0)	2860 ± 654 (1.2)

Fold resistance is given in parenthesis. For experimental details see Section 2.

2.14. Statistical analysis

We used a one-tail paired Student's *t*-test to examine the significance of the difference between two populations for a certain variable. A difference between the averages of two populations was considered significant if the *P*-value obtained was <0.05.

3. Results

3.1. Marked cross-resistance of A549/K1.5 cells to the established ABCG2 substrates mitoxantrone and SN-38

The molecular basis of acquired resistance to C-1305 in A549/K1.5 cells was first explored. A comparison of the chemical structures revealed a substantial structural similarity of C-1305 and its chromophoric homologue, imidazoacridone C-1311 [26] with that of the well-established ABCG2 transport substrate mitoxantrone. We therefore assessed the cross-resistance pattern of A549/K1.5 cells to antitumor agents that are established ABCG2 transport substrates (Table 2A). A549/K1.5 cells displayed 44-fold resistance to C-1305 and 29-fold cross-resistance to its homologue C-1311, relative to parental A549 cells. Moreover, A549/K1.5 cells exhibited a high level of cross-resistance to the well-established ABCG2 substrates mitoxantrone (89-fold) and SN-38 (116-fold), the active metabolite of irinotecan. Consistently, the ABCG2 transport inhibitor fumitremorgin C restored drug sensitivity to these antineoplastic agents. In contrast, A549/K1.5 cells retained parental cell sensitivity to various cytotoxic agents that are not ABCG2 substrates while displaying only a marginal cross-resistance to topoisomerase II inhibitors (Table 2B).

3.2. Expression of ABCG2 and various MDR transporters in A549/K1.5 cells

Consistent with the cross-resistance profile, Western blot analysis revealed a marked ABCG2 overexpression in A549/K1.5 cells, whereas ABCG2 was not detectable in parental A549 cells (Fig. 2A). Reprobing the Western blots with an antibody to the abundant α subunit of Na^+-K^+-ATPase confirmed that equal amounts of proteins were being analyzed (Fig. 2H). The status of expression of various ABC transporters of the MDR family was also examined; equal, albeit substantial protein levels of ABCC1 were present in both parental A549 and A549/K1.5 cells (Fig. 2B). Interestingly, A549/K1.5 cells contained a slight elevation (~3-fold) in the levels of ABCC3 that was barely detectable in parental A549 cells (Fig. 2D). ABCC4 was poorly, yet equally expressed in both parental and A549/K1.5 cells (Fig. 2E). In contrast, ABCC2 (Fig. 2C), ABCC5 (Fig. 2F) and ABCB1 (Fig. 2G) were neither detectable in A549 nor in A549/K1.5 cells.

3.3. Parental cell sensitivity of MRP3 overexpressing cells to C-1305

In order to rule out the possibility that the slightly elevated levels of ABCC3 (shown in Fig. 2) play a contributing role in C-1305 resistance, the well established human ovarian carcinoma cell line 2008 and its ABCC3 (MRP3) overexpressing 2008/MRP3 subline [19] were exposed to various concentrations of C-1305. Results indicated that parental 2008 cell sensitivity to C-1305 (IC_{50} (nM) = 708 ± 201) was retained in 2008/MRP3 cells (IC_{50} (nM) = 796 ± 86).

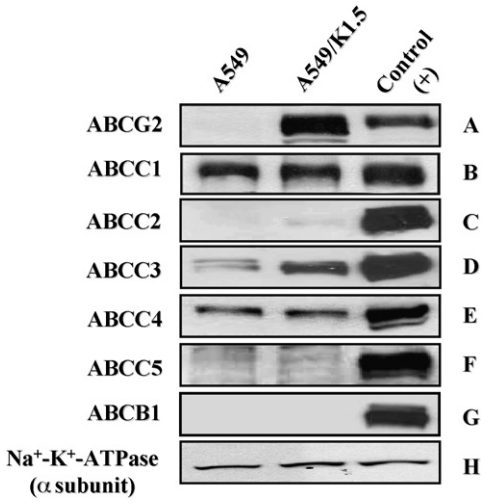

Fig. 2 – Expression levels of ABCG2 and various MDR transporters in parental A549 and A549/K1.5 cells by Western blot analysis. Triton X-100-soluble membrane proteins (50 μg) were resolved by electrophoresis on polyacrylamide gels containing SDS, electroblotted onto Protran BA83 cellulose nitrate membranes and reacted with monoclonal antibodies to ABCG2 (A), ABCC1 (B), ABCC2 (C), ABCC3 (D), ABCC4 (E), ABCC5 (F) and ABCB1 (G). Blots were reprobed with an affinity-purified polyclonal antiserum to the α subunit of Na^+-K^+-ATPase (H). Blots were then reacted with a second horseradish peroxidase (HRP)-conjugated antibody and these nylon membranes were developed using a standard ECL procedure. The right most lane contains protein extracts (50 μg) from the following ABC transporter overexpressing cell lines, used as positive controls: HEK293/ABCG2 (A), 2008/MRP1 (B), 2008/MRP2 (C), 2008/MRP3 (D), HEK293/MRP4 (E), HEK293/MRP5 (F) and AA8/EMT^{R1} (G).

3.4. Plasma membrane overexpression of ABCG2 and exclusion of the chromophore C-1311 in A549/K1.5 cells

The sub-cellular localization of ABCG2 in A549/K1.5 cells was studied by immunohistochemistry (Fig. 3A and B). Monolayers of A549/K1.5 (Fig. 3A) and parental A549 cells (Fig. 3B) were fixed and reacted with an ABCG2 specific antibody (BXP-53) as previously described [22,23]. An intense plasma membrane staining along with some cytoplasmic staining were observed in A549/K1.5 cells (Fig. 3A), whereas none could be detected in parental A549 cells (Fig. 3B). To corroborate these findings we utilized a phycoerythrin (i.e. with red fluorescence) conjugated second antibody after incubation with the 5D3 monoclonal antibody which recognizes an extracellular epitope of ABCG2 on the surface of viable cells [27]; this was combined with a co-incubation with C-1311, a green fluorescent analogue of C-1305 which efficiently intercalates into the DNA [28,29].

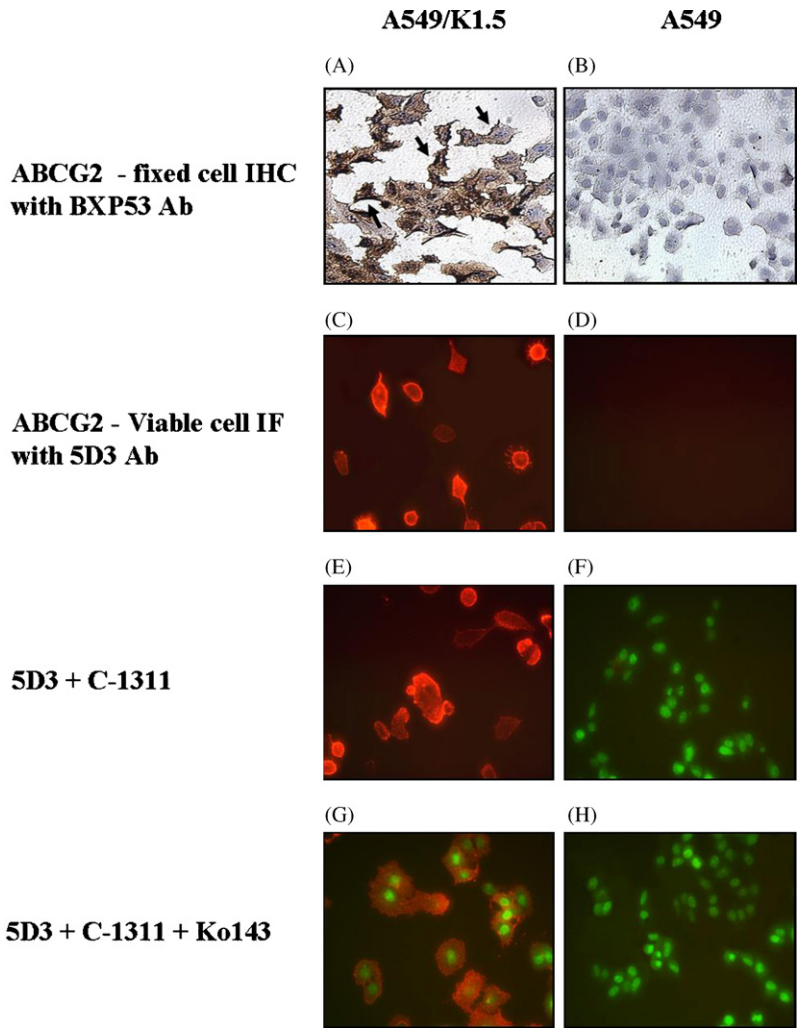

Fig. 3 – Plasma membrane localization of an overexpressed functional ABCG2 in A549/K1.5 cells as revealed by immunohistochemistry, surface 5D3 antibody immunofluorescence and C-1311 fluorescence. Immunohistochemical (IHC) detection of plasma membrane expression of ABCG2 in monolayers of A549/K1.5 (A) and A549 cells (B) was performed after fixation of the cells. A portion of viable A549/K1.5 (C) and A549 cells (D) was incubated with a phycoerythrin-conjugated 5D3 antibody against ABCG2. Another portion of viable A549/K1.5 (E) and A549 cells (F) was incubated for 1 h with 10 μM C-1311 prior to antibody incubation in the absence (E and F) or presence (G and H) of the ABCG2 transport inhibitor Ko143 (0.6 μM) and examined by immunofluorescence (IF) microscopy.

Consistent with the immunohistochemistry results, A549/K1.5 cells displayed an intense red immunofluorescence of ABCG2 at the plasma membrane (Fig. 3C), whereas parental A549 cells were devoid of any staining (Fig. 3D). Likewise, A549/K1.5 cells completely lacked the green nuclear fluorescence of C-1311 (Fig. 3E), which was brightly present in the nuclei of parental A549 cells (Fig. 3F). Furthermore, co-incubation with the potent and specific ABCG2 transport inhibitor Ko143 [30] resulted in the restoration of nuclear green fluorescence in A549/K1.5 cells without affecting their bright red ABCG2 plasma membrane fluorescence (Fig. 3G). In contrast, the fluorescence pattern of parental A549 cells lacking ABCG2 expression but containing brightly green fluorescent nuclei was retained in the presence of Ko143 (Fig. 3H).

3.5. *Lack of C-1305 and C-1311 accumulation in A549/K1.5 cells due to increased ABCG2-dependent drug efflux*

In order to quantify the drug efflux capacity as well as the dose- and time-dependent accumulation of C-1305 in A549 and A549/K1.5 cells, a spectrophotometric assay was employed. A549/K1.5 cells exhibited a significantly decreased C-1305 accumulation, whereas parental A549 cells displayed a dose-dependent accumulation of C-1305 (Fig. 4A). The decreased accumulation of C-1305 was retained for several hours when A549/K1.5 cells were incubated with 10 μM C-1305 (Fig. 4B). A549 and A549/K1.5 cells were then incubated with 10 μM C-1305 for 3 h following which cells were incubated in a drug-free medium thereby allowing for the efflux of cell-associated drug (Fig. 4C). A549/K1.5 cells displayed a promi-

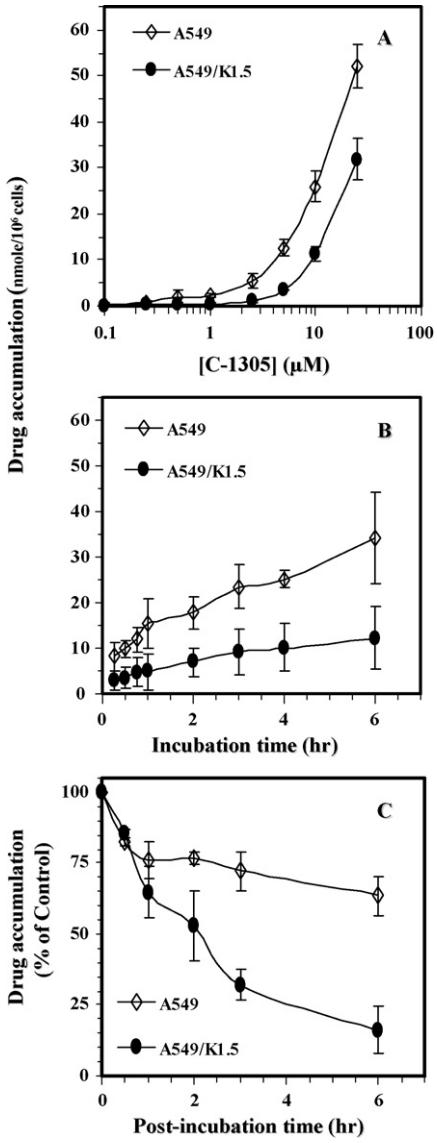

Fig. 4 – Accumulation and efflux of C-1305 in parental and A549/K1.5 cells as determined by a spectrophotometric assay. Cells were incubated for 1 h in various concentrations of C-1305 (A). Another portion of cells was incubated with 10 μM C-1305 for various times (B). Yet another portion of cells was first loaded with 10 μM C-1305 after which the loss of C-1305 via efflux was followed for several hours (C). In all experiments, the amount of C-1305 was determined spectrophotometrically as specified in Section 2.

nent efflux of C-1305 whereas parental cells retained ~70% of the initial drug even after 6 h. These results were consistent with the C-1311 efflux capability of ABCG2 in A549/K1.5 cells using a flow cytometric assay. In this assay, cells were incubated for 1 h in medium containing increasing concentrations of C-1311. Parental A549 cells accumulated C-1311 fluorescence in a dose-dependent manner, whereas A549/K1.5 cells displayed a complete exclusion of C-1311 up to a concentration of 8 μM (Fig. 5A). Co-incubation with Ko143 completely restored C-1311 accumulation in A549/K1.5 cells without affecting chromophore accumulation in A549 cells (Fig. 5B). Moreover, a tight inverse relationship between increased plasma membrane expression of ABCG2 and the level of C-1311 accumulation was observed in A549/K1.5 cells (Fig. 5C). This was consistent with the finding that in the presence of fumitremorgin C, A549/K1.5 cells retained their plasma membrane ABCG2 fluorescence but resumed C-1311 accumulation (Fig. 3G); consequently, the correlation between the two parameters was completely lost (Fig. 5D).

C421 allele-specific ABCG2 gene overexpression in A549/K1.5 cells: In keeping with the marked overexpression of ABCG2 protein in A549/K1.5 cells, real-time PCR and semi-quantitative RT-PCR analyses revealed that ABCG2 mRNA levels were elevated by factors of 30-fold (Fig. 6A) and 32-fold (Fig. 6B), respectively. It is well established that ABCG2 polymorphisms [17,18] and acquired mutations may alter the levels of ABCG2 expression and may augment the levels of drug resistance [20,21,31]. Hence, the nucleotide sequence of ABCG2 cDNA from parental A549 and A549/K1.5 cells was determined. Whereas parental A549 cells contained the frequent A421 single nucleotide polymorphism, A549/K1.5 cells contained only the C421 transcript (Fig. 6C); no other sequence alterations were present in the ABCG2 coding region in A549/K1.5 cells.

3.6. *C421 allele-specific ABCG2 gene amplification in A549/K1.5 cells*

Since markedly elevated ABCG2 mRNA levels may be associated with ABCG2 gene amplification in various malignant cell lines [32–34], ABCG2 gene copy number was determined in A549/K1.5 cells by quantitative genomic PCR (Fig. 7A). A549/K1.5 cells contained a 16-fold ABCG2 gene amplification relative to parental cells. Genomic PCR followed by nucleotide sequencing confirmed that C421 ABCG2 allele-specific gene amplification occurred in A549/K1.5 cells (Fig. 7B). In order to carefully quantify the observed shift in the representation of the C421A allele in A549/K1.5 cells, genomic PCR products containing the C421A polymorphic site were TA-cloned. Thirty-six and 38 genomic clones from A549 and A549/K1.5 cells, respectively, were isolated, sequenced and the frequency of each allele at nucleotide position 421 was determined. Whereas A549 cells retained a near equal clonal distribution of both the wt C421 allele (ratio = 20/36; 55.6%) and the polymorphic A421 ABCG2 allele (ratio = 16/36; 44.4%), A549/K1.5 cells displayed an almost exclusive representation of the wt C421 allele (ratio = 37/38; 97.4%) (Fig. 7C). These results are in full agreement with the C421 allele-specific ABCG2 transcript overexpression in A549/K1.5 cells as revealed by both real-time PCR and semi-quantitative PCR (as shown in Fig. 6).

3.7. *The Q141 ABCG2 confers an increased drug resistance when compared to the K141 ABCG2*

In order to assess the biological advantage of such a selective gene amplification and overexpression of the wt Q141 ABCG2 allele under C-1305 selection, a 72 h growth inhibition assay was carried out. Hence, HEK293 cells and their stable ABCG2 transfectants HEK293/Q141 and HEK293/K141 [18] were

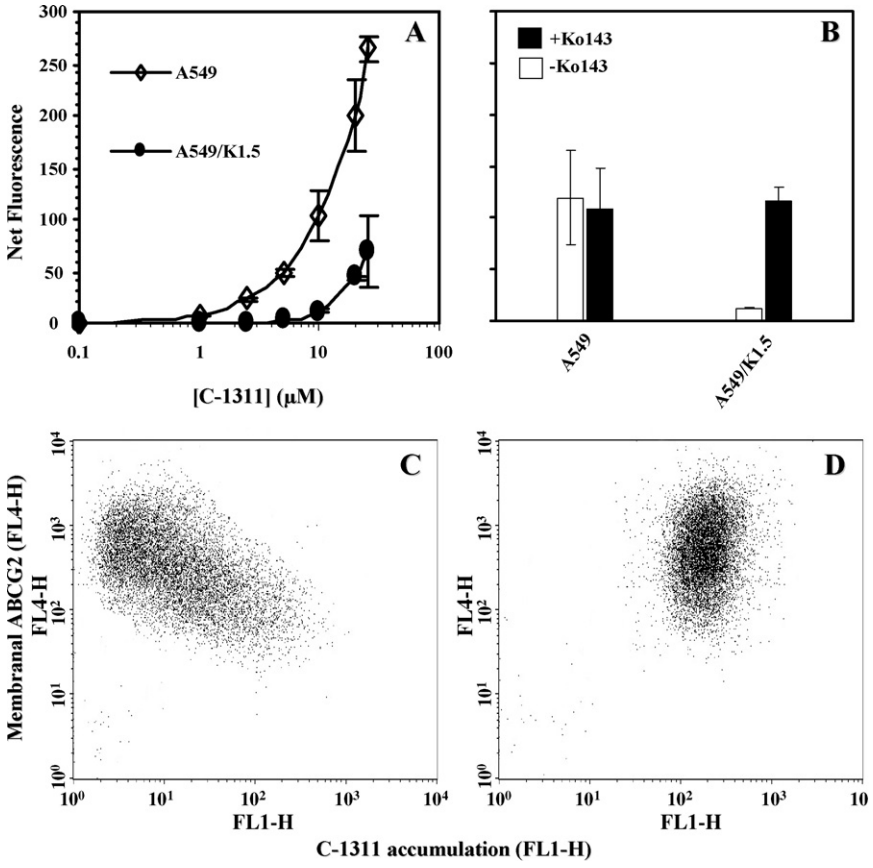

Fig. 5 – Exclusion of C-1311 from A549/K1.5 cells and plasma membrane ABCG2 immunofluorescence in the presence or absence of Ko143 and fumitremorgin C. A549 and A549/K1.5 cells were suspended in a 20 mM HEPES (pH 7.3)-buffered medium containing various C-1311 concentrations ranging from 0.1 μM to 25 μM and incubated for 1 h at 37 °C (A). A portion of these cells was incubated with 10 μM C-1311 in the absence or presence of 0.6 μM Ko143 for 1 h at 37 °C (B). Another portion of A549/K1.5 cells was pre-incubated with 10 μM C-1311 for 1 h followed by a 30 min incubation at 4 °C with an allophycocyanin-conjugated-5D3 monoclonal antibody in the absence (C) or presence of 5 μM fumitremorgin C (FTC) (D). Cells were then analyzed for green and blue fluorescence per cell by flow cytometry.

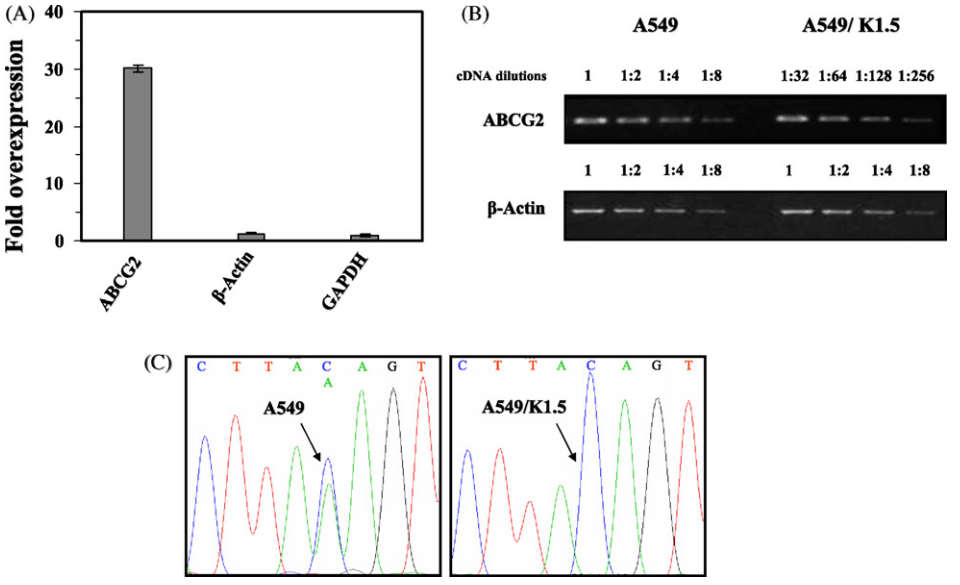

Fig. 6 – Determination of ABCG2 mRNA levels in parental and C-1305-resistant cells by RT-PCR and real-time RT-PCR. ABCG2 transcript levels were quantified using real time RT-PCR analyses (A) and semi-quantitative RT-PCR (B). The C421A and C421 transcripts variants in A549 and A549/K1.5 cells after nucleotide sequencing of the cDNA are shown (C).

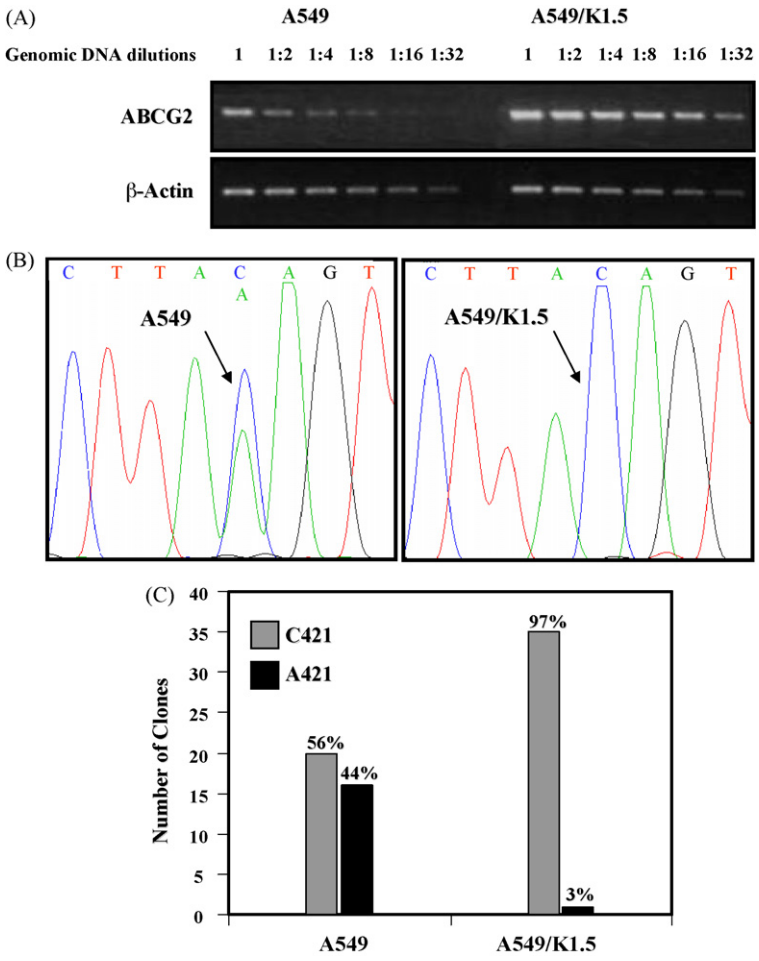

Fig. 7 – Determination of ABCG2 gene copy number in parental A549 and A549/K1.5 cells by quantitative genomic PCR analysis and genomic sequencing of C421 and A421 positive clones. High molecular weight DNA was extracted from A549 and A549/K1.5 cells and the ABCG2 gene copy number was estimated using quantitative genomic PCR with various dilutions of the genomic DNA (A). Nucleotide sequencing was also undertaken in order to verify the C421 allele amplification (B). Quantitative analysis of allele distribution was measured by means of TA-cloning (C).

exposed to various concentrations of C-1305, C-1311 and mitoxantrone. HEK293/Q141 cells overexpressing the wt ABCG2 displayed a marked level of cross-resistance to all three agents, relative to untransfected HEK293 cells (Table 3). Interestingly, the HEK293/K141 displayed a low level of cross-resistance to these drugs, relative to HEK293 cells (Table 3). These results establish a distinct drug resistance advantage for the wt C421 ABCG2 relative to the K141 ABCG2 as manifested by the increased resistance of ~4-, 5- and 5-fold to C-1305, C-1311 and mitoxantrone, respectively (fold resistance P-values of 0.027, 0.039 and 0.007, respectively).

3.8. *Decreased C-1311 drug accumulation in wt ABCG2 HEK293/Q141 cells relative to the polymorphic ABCG2 overexpressing HEK293/K141 transfectants*

The increased resistance pattern achieved by the wt Q141 ABCG2 relative to the polymorphic K141 ABCG2, prompted us

Table 3 – Summary of growth inhibition studies on the HEK293 cell line and its ABCG2 (Q141)- and (K141) stably transfected HEK293/Q141 and HEK293/K141 sublines upon 72 h exposure to C-1305, C-1311 and mitoxantrone

Drug	IC_{50} (nM)		
	HEK293	HEK293/Q141	HEK293/K141
C-1305	209 ± 113 (1.0)	2113 ± 226 (10.1)	584 ± 37 (2.8)
C-1311	33 ± 4.7 (1.0)	523 ± 75 (15.7)	110 ± 2 (3.3)
Mitoxantrone	2.2 ± 0.3 (1.0)	121 ± 5 (55.4)	25 ± 1.8 (11.3)

Fold resistance is given in parenthesis.

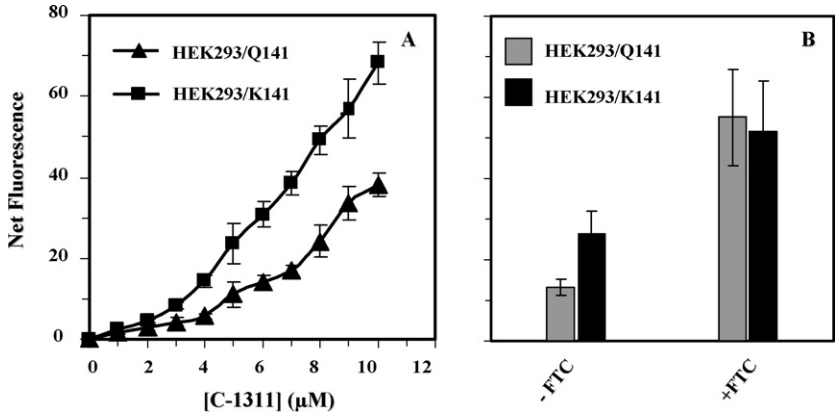

Fig. 8 – C-1311 accumulation in HEK293 cells transfected either with the wt Q141 ABCG2 or the polymorphic K141 ABCG2. HEK293/Q141 and HEK293/K141 cells overexpressing the wt ABCG2 and polymorphic ABCG2 alleles, respectively, were suspended in a 20 mM HEPES (pH 7.3)-buffered medium containing various C-1311 concentrations ranging from 0.1 μM to 10 μM and incubated for 1 h at 37 °C (A). A portion of these cells was incubated with 5 μM C-1311 in absence or presence of 5 μM fumitremorgin C (FTC) for 1 h at 37 °C (B).

to further explore the ability of the two ABCG2 alleles in the extrusion of these acridone agents. HEK293/Q141 and HEK293/K141 cells were thus incubated for 1 h in medium containing increasing concentrations of C-1311 followed by flow cytometric analysis. Both cell lines accumulated C-1311 in a dose-dependent manner; however, the wt ABCG2 overexpressing HEK293/Q141 cells maintained a ~2-fold decreased accumulation of C-1311, relative to the polymorphic K141-ABCG2 overexpressing HEK293/K141 cells (Fig. 8A). Furthermore, whilst at a 5 μM extracellular concentration of C-1311, the two cell lines maintained this statistically significant two-fold accumulation difference (*P*-value = 0.0106), co-incubation with fumitremorgin C increased C-1311 accumulation in both ABCG2 alleles transfected cell lines to a relatively equal high level (*P*-value = 0.3844) (Fig. 8B).

4. Discussion

The current study provides several lines of evidence that wt ABCG2 overexpression is an efficient means of acquisition of drug resistance to the novel antitumor agent C-1305: (a) the genomic ABCG2 locus underwent a marked allele-specific gene amplification as a result of stepwise selection to C-1305. Gene amplification particularly following stepwise drug selection has been one of the hallmarks of drug resistance; (b) A549/K1.5 cells displayed a high level ABCG2 overexpression associated with a markedly decreased accumulation of both the triazoloacridone C-1305 and its imidazoacridone C-1311 chromophoric derivative. Consistently, plotting the plasma membrane ABCG2 levels of individual viable cells versus their cellular C-1311 accumulation revealed a tight correlation with an inverse relationship. Co-incubation with Ko143 and fumitremorgin C restored C-1311 accumulation in A549/K1.5 cells and abolished this inverse correlation with ABCG2 plasma membrane levels. These results establish that C-1311 is efficiently extruded via the MDR efflux transporter ABCG2 that is inhibitable by the potent efflux inhibitors Ko143 and fumitremorgin C. These findings may also have important implications for the future clinical application of C-1311 (Symadex), which is currently undergoing phase II clinical trials as an antitumor drug with selective activity toward colon cancer; (c) A549/K1.5 cells with ABCG2 overexpression exhibited a high level of resistance to well established ABCG2 substrates including mitoxantrone and SN-38 as well as to C-1305 and C-1311; fumitremorgin C restored drug sensitivity to all these ABCG2 substrates. In contrast, A549/K1.5 cells largely retained parental sensitivity to various antitumor agents that are not ABCG2 substrates; (d) wild type ABCG2 transfectants HEK293/Q141 displayed a high level of cross-resistance to C-1305 and C-1311 when compared to their untransfected HEK293 counterpart, thereby confirming the pivotal role that ABCG2 plays in drug resistance to these cytotoxic agents; (e) immunofluorescence microscopy detection of ABCG2 in live cells along with C-1311 chromophore accumulation revealed a predominant plasma membrane localization of ABCG2 accompanied by a complete exclusion of this fluorochrome from A549/K1.5 cells. In contrast, parental A549 cells lacking ABCG2 expression displayed an intense chromophore accumulation and a consequent nuclear staining which is consistent with C-1311 being a potent DNA intercalator [28,29]. Expectedly, disruption of ABCG2 efflux activity by Ko143 restored chromophore accumulation as manifested by the bright nuclear staining in A549/K1.5 cells.

Parental A549 cells harbor a heterozygous C421A ABCG2 genotype that has been identified as a frequent single nucleotide polymorphism [17]. In contrast, TA-cloning of genomic PCR ABCG2 products followed by DNA sequencing as well as DNA sequence analysis after comparative RT- and real-time PCR revealed that A549/K1.5 cells contained a marked C421 ABCG2 allele-specific gene amplification and a consistent overproduction of this C421 ABCG2 transcript. Moreover, growth inhibition and accumulation assays using the parent C-1305 and its C-1311 homologue with the transfected C421- and A421 ABCG2 alleles provided evidence for a significant drug resistance advantage favoring the wt Q141 ABCG2 over

the K141 variant. These results suggest that during the stepwise selection with C-1305, a monoallelic C421 ABCG2 gene amplification occurred which conferred a drug resistance advantage via active drug extrusion. Consistently, recently it was shown that the A421 ABCG2 allele is tightly associated with a poor overall expression of the encoded K141 ABCG2 protein variant as well as with a substantial increase in its cytoplasmic localization. Moreover, even at comparable plasma membrane levels of ABCG2, the K141 protein conferred a significantly decreased resistance level towards established ABCG2 substrates including mitoxantrone, topotecan and SN-38 due to diminished efflux capabilities [18]. In contrast, the wt C421 ABCG2 allele supported the expression of large amounts of the highly functional Q141 ABCG2 located predominantly in the plasma membrane, thereby facilitating cellular resistance to multiple anticancer drugs. Our results indicate that although an A421 allele-specific ABCG2 gene amplification could have occurred during the early stages of C-1305 selection, it could only support an inferior level of drug resistance when compared to the Q141 ABCG2. According to this scenario, individual cells with a low level of C421 ABCG2 allele-specific amplification could have undergone clonal expansion under the gradually increasing cytotoxic selection with C-1305. Our present finding of allele-specific ABCG2 gene amplification gains a strong support from a recent study in which a novel genome wide allele-specific copy number analysis has been devised using a probe-level allele-specific quantification procedure [35]. Applying this novel method to a collection of lung cancer samples showed that genomic amplifications are monoallelic, as would be expected from the mechanisms currently believed responsible for gene amplification [36] including unequal sister chromatid exchange [37]. However, in our study, whether or not allele-specific ABCG2 gene amplification is indeed the result of unequal sister chromatid exchange or another mechanism must await further investigation. Hence, monoallelic amplifications are one of the hallmarks of cancers, which equip malignant cells with growth advantages including anticancer drug resistance.

The imidazoacridone (C-1311) and triazoloacridone (C-1305) antineoplastic agents studied here possess lipophilic characteristics, which may have important implications for the mechanism of anticancer drug extrusion mediated by the ABCG2 efflux transporter. First, C-1311 and C-1305 have calculated log *P* values (i.e. log value of octanol: water partition coefficient) of 3.97 and 1.37, respectively. Second, at physiological pH, C-1311 is also present as a positively charged amphipathic compound. Hence, these characteristics imply that the predicted partitioning of these acridones into the plasma membrane would be up to 10,000-fold better than their solubility in the aqueous phase (i.e. extracellular medium and cytosol). Indeed, recent studies have demonstrated that the structurally related compound mitoxantrone partitions 230,000-fold better in lipid membranes than in the aqueous milieu [38]. In fact, this membrane partitioning of mitoxantrone exceeds by far the partitioning that would have been predicted from its log *P* value. Although hydrophobic, the positive charge of C-1311 would presumably allow its insertion at the outer leaflet of the plasma membrane among the phospholipid head groups as has been shown for mitoxantrone and other anthracyclines [38]. Thus, the relatively slow flip-flop events are the driving force and the rate-limiting step in the transmembrane movement and the traverse of the membrane by such hydrophobic cationic acridone and anthracenedione derivatives. Based on these characteristics, once the acridone drug is present at the hydrophilic extracellular milieu, it would display a 10,000-fold preferential co-partitioning into the outer leaflet of the plasma membrane. Consequently, the acridone residence time at the plasma membrane is expected to be relatively long when considering its structural homologue mitoxantrone [38]. It is likely that the highly overexpressed ABCG2 at the plasma membrane of A549/K1.5 cells recognizes lipophilic acridone derivatives within the lipid bilayer and extrudes them out of cells even before they could traverse the plasma membrane into the cytosol. According to this paradigm that has been first suggested for ABCB1 [39] and recently for ABCG2 [21], the latter transporter does not need to bear a high affinity for such acridone substrates as their intramembranal concentrations may easily reach the millimolar range even when present at sub-micromolar concentrations in the extracellular medium [21].

Acknowledgments

Grant support: The Fred Wyszkowski Cancer Research Fund (to YGA) and the Polish Ministry of Scientific Research and Information Technology, grant no 2P05F 01429 (to AS).

We thank Dr. G.L. Scheffer and Prof. R.J. Scheper (Dept. of Pathology, VU University Medical Centre, Amsterdam, The Netherlands) for generously providing monoclonal antibodies to the various MDR transporters, Prof. A.H. Schinkel for the kind gift of Ko143, and Prof. S.J. Karlish (Dept. of Biological Chemistry, The Weizmann Institute of Science, Rehovot, Israel) for the polyclonal antiserum against Na^+-K^+-ATPase. We also thank Marcin Wojciechowski for assistance with log *P* values determination.

REFERENCES

[1] Cholody WM, Martelli S, Konopa J. 8-substituted 5-[(aminoalkyl)amino]-6H-v-triazolo[4,5,1-de]acridin-6-ones as potential antineoplastic agents. Synthesis and biological activity. J Med Chem 1990;33:2852–6.
[2] Kusnierczyk H, Cholody WM, Paradziej-Lukowicz J, Radzikowski C, Konopa J. Experimental antitumor activity and toxicity of the selected triazolo- and imidazoacridones. Arch Immunol Ther Exp (Warsz) 1994;42:415–23.
[3] Lemke K, Poindessous V, Skladanowski A, Larsen AK. The antitumor triazoloacridone C-1305 is a topoisomerase II poison with unusual properties. Mol Pharmacol 2004;66:1035–42.
[4] Vogelstein B, Kinzler KW. Cancer genes and the pathways they control. Nat Med 2004;10:789–99.
[5] Lemke K, Wojciechowski M, Laine W, et al. The antitumor triazoloacridone C-1305 is a topoisomerase II poison with unusual properties. Nucleic Acids Res 2005;33:6034–47.
[6] Borst P, Elferink RO. Mammalian ABC transporters in health and disease. Annu Rev Biochem 2002;71:537–92.
[7] Ambudkar SV, Kimchi-Sarfaty C, Sauna ZE, Gottesman MM. P-glycoprotein: from genomics to mechanism. Oncogene 2003;22:7468–85.

[8] Sarkadi B, Özvegy-Laczka O, Nemet K, Varadi A. ABCG2-a transporter for all seasons. FEBS Lett 2004;567:116–20.
[9] Szakacs G, Paterson JK, Ludwig JA, Booth-Genthe C, Gottesman MM. Targeting multidrug resistance in cancer. Nat Rev Drug Discov 2006;5:219–34.
[10] Deeley RG, Westlake C, Cole SP. Transmembrane transport of endo- and xenobiotics by mammalian ATP-binding cassette multidrug resistance proteins. Physiol Rev 2006;86:849–99.
[11] Krishnamurthy P, Schuetz JD. Role of ABCG2/BCRP in biology and medicine. Ann Rev Pharmacol Toxicol 2006;46:381–410.
[12] Cervenak J, Andrikovics H, Ozvegy-Laczka C, et al. The role of human ABCG2 multidrug transporter and its variants in cancer therapy and toxicology. Cancer Lett 2006;234:62–72.
[13] Assaraf YG. The role of multidrug resistance efflux transporters in antifolate resistance and folate homeostasis. Drug Resist Update 2006;9:227–46.
[14] Dean M, Harmon Y, Chimini G. The human ATP-binding cassette (ABC) transporter superfamily. J Lipid Res 2001;42:1007–17.
[15] Haimeur A, Conseil G, Deeley RG, Cole SP. The MRP-related and BCRP/ABCG2 multidrug resistance proteins: biology, substrate specificity and regulation. Curr Drug Metab 2004;5:21–53.
[16] Kruh GD, Belinsky MG. The MRP family of drug efflux pumps. Oncogene 2003;22:7535–52.
[17] Imai Y, Nakane M, Kage K, et al. C421 polymorphism in the human breast cancer resistance protein gene is associated with low expression of Q141K protein and low level drug resistance. Mol Cancer Ther 2002;1:611–6.
[18] Morisaki K, Robey RW, Özvegy-Laczka C, et al. Single nucleotide polymorphisms modify the transporter activity of ABCG2. Cancer Chemother Pharmacol 2005;56:161–72.
[19] Kool M, van der Linden M, de Haas M, et al. MRP3, an organic anion transporter able to transport anticancer drugs. Proc Natl Acad Sci USA 1999;96:6914–9.
[20] Shafran A, Ifergan I, Bram E, et al. ABCG2 harboring the Gly482 mutation confers high level resistance to hydrophilic antifolates. Cancer Res 2005;65:8414–22.
[21] Bram E, Ifergan I, Shafran A, Berman B, Jansen G, Assaraf YG. Mutant Gly482 and Thr482 ABCG2 mediate high-level resistance to lipophilic antifolates. Cancer Chemother Pharmacol 2006;58:826–34.
[22] Ifergan I, Shafran A, Jansen G, Hooijberg JH, Scheffer GL, Assaraf YG. Folate deprivation results in the loss of breast cancer resistance protein (ABCG2) expression: a role for BCRP in cellular folate homeostasis. J Biol Chem 2004;279:25527–34.
[23] Ifergan I, Jansen G, Assaraf YG. Cytoplasmic confinement of breast cancer resistance protein (BCRP/ABCG2) as a novel mechanism of adaptation to short-term folate deprivation. Mol Pharmacol 2005;4:1–11.
[24] Poindessous V, Koeppel F, Raymond E, Comisso M, Waters S, Larsen AK. Marked activity of irofulven (MGI-114) toward human carcinoma cells: comparison with cisplatin and ecteinascidin (ET-743). Clin Cancer Res 2003;9:2817–25.
[25] Hilal SH, Karickhoff SW, Carreira LA. Verification and validation of the SPARC Model. U.S. Environmental Protection Agency, Athens, GA 2003; publication No. EPA/600/R-03/03.
[26] Cholody WM, Martelli S, Paradziej-Lukowicz J, Konopa J. 5-[(Aminoalkyl)amino]imidazo[4,5,1-de]acridin-6-ones as a novel class of antineoplastic agents. Synthesis and biological activity. J Med Chem 1990;33:49–52.
[27] Zhou S, Schuetz JD, Bunting KD, et al. The ABC transporter Bcrp1/ABCG2 is expressed in a wide variety of stem cells and is a molecular determinant of the side population phenotype. Nat Med 2001;7:1028–34.
[28] Berger B, Marquardt H, Westendorf J. Pharmacological and toxicological aspects of new imidazoacridone antitumor agents. Cancer Res 1996;56:2094–104.
[29] Dziegielewski Z, Slusarski B, Konitz A, Skladanowski A, Konopa J. Intercalation of imidazoacridones to DNA and its relevance to cytotoxic and antitumor activity. Biochem Pharmacol 2002;63:1653–62.
[30] Allen JD, van Loevezijn A, Lakhai JM, et al. Potent and specific inhibition of breast cancer resistance protein multidrug transporter *in vitro* and in mouse intestine by a novel analogue of fumitremorgin C. Mol Cancer Ther 2002;1:417–25.
[31] Robey RW, Honjo Y, Morisaki K, et al. Mutations at amino-acid 482 in the ABCG2 gene affect substrate and antagonist specificity. Br J Cancer 2003;89:1971–8.
[32] Allen JD, Brinkhuis RF, Wijnholds J, Schinkel AH. The mouse Bcrp1/Mxr/Abcp gene: amplification and overexpression in cell lines selected for resistance to topotecan, mitoxantrone, or doxorubicin. Cancer Res 1999;59:4237–41.
[33] Volk EL, Farley KM, Wu Y, Li F, Robey RW, Schneider E. Overexpression of wild type breast cancer resistance protein mediates methotrexate resistance. Cancer Res 2002;62:5035–40.
[34] Rao VK, Wangsa D, Robey RW, et al. Characterization of ABCG2 gene amplification manifesting as extrachromosomal DNA in mitoxantrone-selected SF295 human glioblastoma cells. Cancer Genet Cytogenet 2005;160:126–33.
[35] LaFramboise T, Weir BA, Zhao X, et al. Allele-specific amplification in cancer revealed by SNP array analysis. PLoS Comput Biol 2005;1:507–17.
[36] Albertson GD. Gene amplification in cancer. Trends Genet 2006;22:447–55.
[37] Herrick J, Conti C, Teissier T, et al. Genomic organization of amplified MYC genes suggests distinct mechanisms of amplification in tumorigenesis. Cancer Res 2005;65:1174–9.
[38] Regev R, Yeheskely-Hayon D, Katzir H, Eytan GD. Transport of anthracyclines and mitoxantrone across membranes by a flip-flop mechanism. Biochem Pharmacol 2005;70:161–9.
[39] Higgins CF, Gottesman MM. Is the multidrug resistance a flippase? Trends Biochem Sci 2002;17:18–21.